APPLICATION OF DIFFERENT HIGH-ORDER BOUNDARY CONDITIONS TO CRYSTAL PLASTICITY

Eduardo Bittencourt

Departamento de Engenharia Civil, Universidade Federal do Rio Grande do Sul, Av. Osvaldo Aranha, 99, sala 308-a, Porto Alegre. 90035-190, RS, Brazil, eduardo.bittencourt@ufrgs.br.

Keywords: Crystal Plasticity, dislocations, boundary conditions.

Abstract. When Burgers vector is accounted for in crystal plasticity theories through energetic dependences, high-order boundary conditions are required. In the work done by Gurtin and Needleman (*J. Mech. Phys. Solids*, 53:1-31 (2005)) is shown that a boundary condition based directly on slip-rates is inappropriate for being too restrictive. The authors suggest a new type of boundary condition based on the flow of the Burgers vector. In the present work, the two types of boundary conditions are implemented in a finite element crystal plasticity code. Only small-deformation and 2D cases are considered. Details about the new formulation are commented. The boundary conditions are tested considering a single crystal and hard surfaces. Preliminary results show that the use of the second type of high-order boundary condition leads to more adequate results than the first type, when compared to discrete dislocation results.

1 INTRODUCTION

The consideration of the effects of geometrically necessary dislocations (Nye, 1953; Ashby, 1970) gives rise to a material response that is size dependent, as observed in experiments (Fleck et al.,1994). Nonlocal crystal plasticity theories that take into account these dislocations have been proposed in the last few years. These theories can be broadly separated in two categories: those that consider higher-order terms (e.g. Shu and Fleck, 1999; Gurtin, 2002) and those that do not (e.g. Acharya and Bassani, 2000). While lower-order theories are much simpler to implement in an existing conventional plasticity code, in some cases, such as the development of boundary layers (Shu et al., 2001), these theories fail to reproduce material behavior. On the other side, higher-order theories may introduce difficulties to regard boundary conditions.

In order to take into account higher-order terms, additional degrees of freedom should be considered. This constraint leads to mixed formulations. In the present work the theory of Gurtin (2002) will be followed. As a consequence, besides displacements, crystal slips are considered independent variables. Originally the theory established higher-order boundary conditions in terms of slip-rates. In Gurtin and Needleman (2005), however, it is demonstrated that a boundary condition based directly on slip-rates leads to uniqueness problems. The authors then establish uniqueness conditions when higher-order boundary conditions are formulated in terms of the flow of the Burgers vector.

In section 2, details of the theory of Gurtin (2002) are given as well as the modifications introduced by Gurtin and Needleman (2005). In section 3, a boundary value problem for a single crystal is considered: a model composite material is subjected to simple shear. Elastic rectangular particles are embedded in a plastically deforming matrix. The different possible higher-order boundary conditions are numerically tested at the matrix/particle boundaries. Final remarks are presented in section 4.

2 CRISTAL PLASTICITY FORMULATION

The gradient of the displacement vector, $u_{i,j}$, is written as the sum of an elastic u_{ij}^e and a plastic u_{ij}^p part. The plastic part occurs by crystallographic slip on a set of slip planes. With $s_i^{(\beta)}$ and $m_i^{(\beta)}$ unit vectors specifying the slip direction and the slip plane normal, respectively, for slip on a system β, the plastic part of the displacement gradient is given by

$$u_{ij}^p = \sum_\beta \gamma^{(\beta)} s_i^{(\beta)} m_j^{(\beta)} \tag{1}$$

with $\gamma^{(\beta)}$ the total slip on the system β. Greek superscripts, with no summation convention, are used to label the slip systems. We consider slip system directions fixed throughout calculations.

In the case of Gurtin (2002), with body forces neglected, the principle of virtual work can be written as

$$\int_B \left[\sigma_{ij}\delta u_{i,j} + \sum_\beta \left(\pi^{(\beta)} - \tau^{(\beta)}\right)\delta\gamma^{(\beta)} + \sum_\beta \xi_i^{(\beta)}\delta\gamma_{,i}^{(\beta)} \right]dV =$$

$$\int_{\partial B_q} \sum_\beta q^{(\beta)}\delta\gamma^{(\beta)}dA + \int_{\partial B_t} t_i\delta u_i dA. \tag{2}$$

Here, $t_i = \sigma_{ij}n_j$, $q^{(\beta)} = \xi_i^{(\beta)}n_i$ where n_i is the surface normal, ∂B_t is the part of the boundary on which t_i is prescribed, ∂B_q is the part of the boundary on which $q^{(\beta)}$ is prescribed and

$$\tau^{(\beta)} = P_{ij}^{(\beta)}\sigma_{ij} \quad , \quad P_{ij}^{(\beta)} = \frac{1}{2}\left(s_i^{(\beta)}m_j^{(\beta)} + s_j^{(\beta)}m_i^{(\beta)}\right). \tag{3}$$

The quantities $\pi^{(\beta)}$ and $\xi_i^{(\beta)}$ are specified through constitutive relations. The macro boundary conditions are that at each point on the boundary either t_i or u_i is prescribed and the corresponding micro boundary conditions are that either $q^{(\beta)}$ or $\gamma^{(\beta)}$ is prescribed as follows:

- Microscopically hard boundary conditions: surface is hard in the sense that dislocations do not pass through it. It characterizes for instance the boundary behavior of the crystal bonded perfectly to a non-metalic surface. In this case:

$$\gamma^{(\beta)} = 0 \tag{4}$$

- Microscopically free boundary conditions: characterizes the boundary behavior where the environment excerts no forces impending slip on slip system (β). In this case:

$$\xi_i^{(\beta)} n_i = 0 \tag{5}$$

Since Eq. (2) holds for independent variations in δu_i and $\delta\gamma^{(\beta)}$, we can separate the principle of virtual work in two parts as

$$\int_B \sigma_{ij}\delta u_{i,j}dV = \int_{\partial B_t} t_i\delta u_i dA \tag{6}$$

and

$$\int_B \Big[\sum_\beta \left(\pi^{(\beta)} - \tau^{(\beta)}\right)\delta\gamma^{(\beta)} + \sum_\beta \xi_i^{(\beta)}\delta\gamma_{,i}^{(\beta)} \Big]dV = \int_{\partial B_q} \sum_\beta q^{(\beta)}\delta\gamma^{(\beta)}dA \tag{7}$$

which form the basis of the finite element formulation. The microforce part, Eq. (7) only applies during plastic flow, $\dot\gamma^{(\beta)} \neq 0$. Corresponding classical balance and microforce balance are:

$$\sigma_{ij,j} = 0 \tag{8}$$

and

$$\pi^{(\beta)} - \tau^{(\beta)} - \xi_{i,i}^{(\beta)} = 0. \tag{9}$$

The stress σ_{ij} is given in the rate form

$$\dot\sigma_{ij} = C_{ijkl}\dot u_{k,l} - C_{ijkl}\sum_\alpha \dot\gamma^{(\alpha)}P_{kl}^{(\alpha)} \tag{10}$$

with $(\dot{}) = \partial()/\partial t$, where t is time.

We focus attention on rate independent material behavior and cases where the geometrically necessary dislocations only affect the energetic hardening. We take

$$\pi^{(\beta)} = \sigma^{(\beta)}\mathrm{sgn}\dot\gamma^{(\beta)} \tag{11}$$

with $\sigma^{(\beta)}$ having the initial value σ_0 for all β and and the corresponding $\pi^{(\beta)}$ having the initial value π_0. $\sigma^{(\beta)}$ evolves as

$$\dot\sigma^{(\beta)} = \sum_\alpha h^{(\beta\alpha)}|\dot\gamma^{(\alpha)}| \qquad h^{(\alpha\beta)} = qH_0 + (1-q)H_0\delta_{\alpha\beta} \tag{12}$$

where H_0 is a prescribed constant and q is the latent hardening ratio. The relation (11) applies only when there is flow on slip system β, i.e. when $\dot\gamma^{(\beta)} \neq 0$.

In the case of Gurtin and Needleman (2005), the virtual work associated to microforces is considered a function of the Burgers vector G_{ij}:

$$G_{ij} = \epsilon_{irs} \frac{\partial u^p_{js}}{\partial x_r}. \tag{13}$$

ϵ_{ipq} is the alternating tensor. The work conjugated to G_{ij} is a defect stress T_{ij}. In this case, Eq.(7) can be rewritten as:

$$\int_B \Big[\sum_\beta \left(\pi^{(\beta)} - \tau^{(\beta)} \right) \delta\gamma^{(\beta)} + T_{ij}\delta G_{ij} \Big] dV = \int_{\partial B_Q} Q_{kl}\delta u^p_{kl} dA \tag{14}$$

where,

$$Q_{ij} = T_{ri}\epsilon_{rkj}n_k. \tag{15}$$

Considering that the defect stress T_{ij} is related to micro-stress $\xi^{(\beta)}_i$ by the relation below,

$$\xi^{(\beta)}_i = \epsilon_{ipq}m^{(\beta)}_p T_{rq}s^{(\beta)}_r, \tag{16}$$

the same microforce balance (Eq. 9) is obtained. However Gurtin and Needleman (2005) show that microscopic boundary conditions are not completely equivalente in both virtual work formulations. Considering Eq. (16), (15) and (1) it is easy to show that microscopically free boundary condition $q^{(\beta)} = 0$ is equivalent to $Q_{ij}m_i s_j = 0$ for all (β). However, this is not the case for the microscopically hard boundary condition. From Eq. (14) can be said that this boundary condition is:

$$u^p_{ri}\epsilon_{rkj}n_k = 0 \tag{17}$$

The old microscopically hard boundary condition (Eq. 4) in fact corresponds to $u^p_{ij} = 0$, which is a much more restrictive or stronger than condition in Eq. (17).

As here we confine attention to plane strain calculations, $s^{(\beta)}_3 = 0$ and $m^{(\beta)}_3 = 0$ for all slip systems, the new microscopically hard boundary condition (Eq. 17) corresponds to:

$$\sum_\beta \gamma^{(\beta)} s^{(\beta)}_i (s^{(\beta)}_k n_k) = 0 \qquad (i = 1, 2). \tag{18}$$

Clearly, only slip systems that are orthogonal to the boundary surface ∂B_Q will be completely blocked.

Just complementing the theory, the defect stress is defined as (Gurtin, 2002):

$$T_{ji} = \ell^2 \pi_0 G_{ij}, \tag{19}$$

where ℓ is a material length parameter.

In the next section a two dimensional model composite material subject to simple shear is tested considering the three microscopic boundary conditions discussed in this section. Equations are implemented in a finite element framework, as described in Bittencourt (2012).

3   NUMERICAL EXPERIMENTATION

A planar model composite material consisting of elastic rectangular particles embedded in a plastically deforming matrix is subjected to simple shear as sketched in Fig. 1. The geometrical parameters and the elastic properties of the matrix and of the reinforcement are the same as in
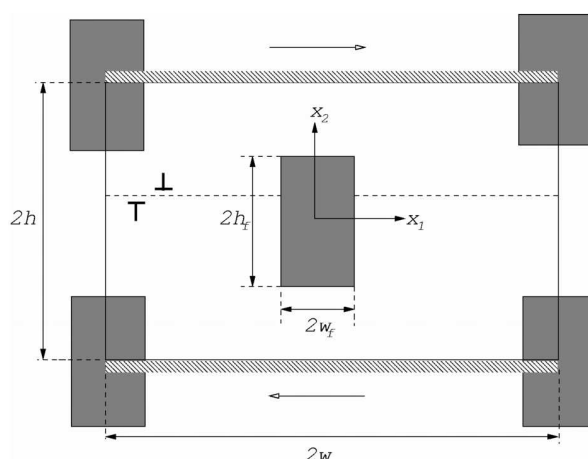
Figure 1: Unit cell of a composite material with a doubly periodic array of elastic particles. Slip planes are parallel to the applied shear direction.

Bittencourt et al.(2003). The matrix material has a single slip system with the shearing direction parallel to the slip plane. the particles are rectangular and do not leave any unreinforced veins of matrix material.

The reinforcing particles are arranged in a hexagonal array, with each unit cell being of width $2w$ and height $2h$ ($w/h = \sqrt{3}$) (see Fig. 1). The particles are of size $2w_{\mathrm{f}} \times 2h_{\mathrm{f}}$; $h_f = 2w_f = 0.588h$. The reinforcement area fraction is 0.2.

The macroscopic boundary conditions on a unit cell are

$$u_1(t) = \pm h\Gamma(t), \quad u_2(t) = 0 \quad \text{along} \quad x_2 = \pm h \tag{20}$$

Along the lateral sides ($x_1 = \pm w$) periodic macro-scale boundary conditions are imposed and the micro-scale boundary condition is taken to be $q^{(1)}(\pm w) = \xi_i^{(1)}(\pm w)n_i = 0$. For comparison purposes, on the reinforcement-matrix interface, three different micro-boundary conditions are tested:

- the micro-free boundary condition $q^{(1)} = 0$;

- the old micro-hard boundary condition $\gamma^{(1)} = 0$;

- the new micro-hard boundary condition Eq.(18). At the vertical interfaces, where slip system is perpendicular to the particle surface, we have $\gamma^{(1)} = 0$. At the horizontal interfaces the micro-hard boundary condition is nonexistent and the result is a micro-free boundary condition $q^{(1)} = 0$.

Each phase is considered to be elastically isotropic, with shear modulus $\mu = 26.3$ GPa and Poisson's ratio $\nu = 0.33$ for the matrix; the corresponding values for the reinforcement are 192.3 GPa and 0.17, respectively. A value of $\sigma_0 = 28$ MPa for the matrix and $h/\ell = 1.25$ was found to give good agreement with the monotonic stress-strain response obtained from the discrete dislocation calculations. A finite element mesh consisting of 384 bi-quadratic elements was used.

Contours of slip, $\gamma^{(1)}$, are shown in Fig. 2, for $\Gamma = 0.0096$ and $H_0 = 0$. Micro-free, the old and new micro-hard boundary conditions are considered (from top to down in the figure, respectively).
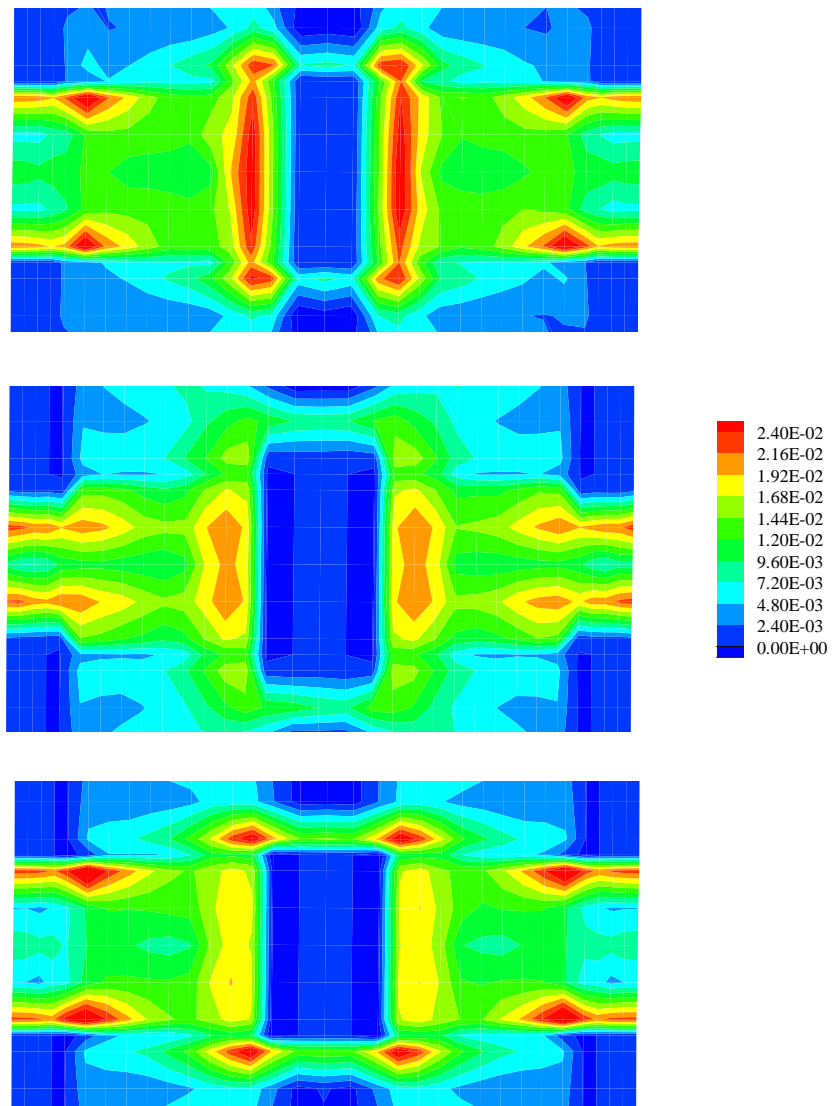
Figure 2: Contours of slip $\gamma^{(1)}$. (above) Micro-free, (midle) old micro-hard and (below) new micro-hard boundary conditions.
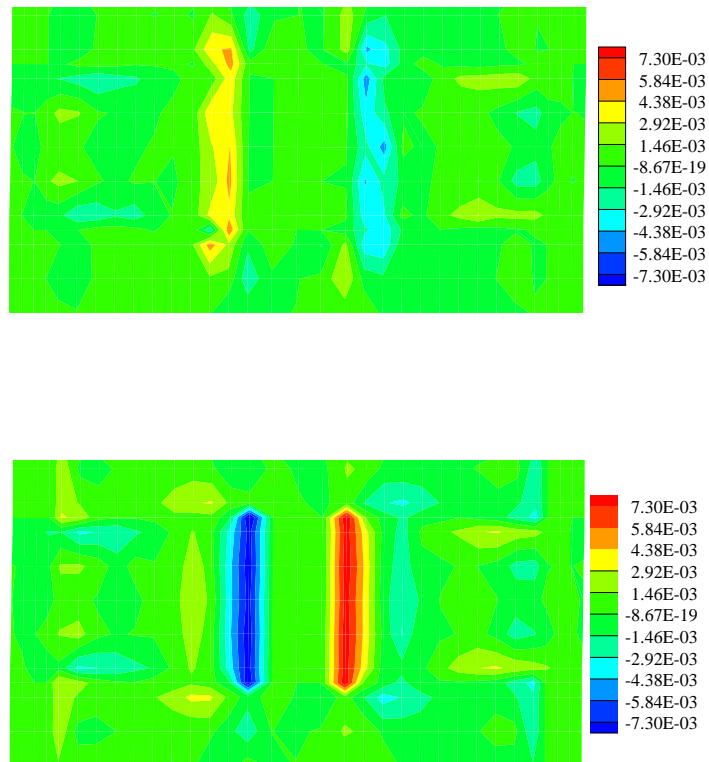
Figure 3: Contours of microstress $\xi_1^{(1)}$. (above) Micro-free, (below) new micro-hard boundary conditions.

For the micro-free case, slip is localized near the central reinforcement, particulary at the vertical interfaces of the particle. On the other hand, for the old micro-hard case, slip is more spread out in the unit cell. Finally, in the new micro-hard case, slip tends to localize at the horizontal interfaces of all particles. This is the only distribution of slips that is consistent with the displacement distributions seen in the discrete dislocation solution shown by Cleveringa et al. (1997).

The slip distribution reflects the rotation of the reinforcement (see Cleveringa et al., 1997), which requires the presence of geometrically necessary dislocations near the reinforcement, Ashby (1970). In Fig. 3(below), with the new micro-hard boundary condition, the contours of micro-stress $\xi_1^{(1)}$ reflect a density of geometrically necessary dislocations at the particle-matrix interface as seen in the discrete dislocation distribution in Cleveringa et al. (1997). For the micro-free boundary condition, Fig. 3(above), the density of geometrically necessary dislocations is much lower and peaks away from the interface.

4   DISCUSSION AND FINAL REMARKS

The new type of higher-order boundary condition developed by Gurtin and Needleman (2005) has been implemented in a finite element framework and tested in a model composite material. Boundary conditions developed previously (Gurtin, 2002) are also considered and compared to the new type. While the micro-free boundary condition is equivalent in both for-

mulations, this is not the case of the micro-hard boundary condition. In the old formulation this condition means that no dislocation can pass through the boundary. In the new formulation the flux of dislocations on boundary depends on the orientation of the slip system with the boundary surface.

The example used to test the new micro-hard boundary condition is appealing because, depending on the surface, two limit situations are found. In the surfaces where slip system is perpendicular to the boundary, dislocations are completely blocked, as in the old micro-hard boundary condition. In the surfaces where slip system is paralel to the boundary, dislocations are completely free to flow, as in the free micro-hard boundary condition. The new micro-hard boundary condition is the only that can match the deformation pattern found in discrete dislocation calculations (Cleveringa et al., 1997).

Distribution of the density of geometrically necessary dislocations (Fig. 3) and average shear stress (not shown in this work) obtained with the new micro-hard boundary condition are also consistent with discrete dislocation results (Cleveringa et al., 1997).

ACKNOWLEDGMENTS

REFERENCES

Acharya A. and Bassani J.L. Incompatibility and crystal plasticity. *J. Mech. Phys. Solids*, 48:1565–1595, 2000.

Ashby M.F. The deformation of plastically non-homogeneous materials. *Phil. Mag.*, 21:399–424, 1970.

Bittencourt E., Needleman A., Gurtin M.E. and Van der Giessen E. A comparison of nonlocal continuum and discrete dislocation plasticity predictions. *J. Mech. Phys. Solids*, 51:281–310, 2003.

Bittencourt E. Numerical solution of crystal plasticity problems by a mixed formulation. *Comp. Mat. Sci.*, 63:145-153, 2012.

Cleveringa H.H.M., Van der Giessen E. and Needleman A. Comparison of discrete dislocation and continuum plasticity predictions for a composite material. *Acta Mater.*, 45:3163–3179, 1997.

Fleck N.A., Muller G.M., Ashby F. and Hutchinson J.W. Strain gradient plasticity: theory and experiment. *Acta Metall. Mater.*, 42:475–487, 1994.

Gurtin M.E. A gradient theory of single-crystal viscoplasticity that accounts for geometrically necessary dislocations. *J. Mech. Phys. Solids*, 50:5–32, 2002.

Gurtin M.E. and Needleman A. Boundary conditions in small-deformations, single-crystal plasticity that account for the Burgers vector. *J. Mech. Phys. Solids*, 53:1–31, 2005.

Nye J.F. Some geometrical relations in dislocated solids, *Acta Metall.*, 1:153–162, 1953.

Shu J.Y., Fleck N.A., Van der Giessen E. and Needleman A. Boundary layers in constrained plastic flow: comparison of nonlocal and discrete dislocation plasticity. *J. Mech. Phys. Solids*, 49:1361–1395, 2001.

Shu J.Y. and Fleck N.A. Strain gradient crystal plasticity: size-dependent deformation of bicrystals. *J. Mech. Phys. Solids*, 47:297–324, 1999.